

Decays of the $T_z = -2$ nuclei ^{20}Mg , ^{24}Si , and ^{36}Ca

J. Äystö,* M. D. Cable, R. F. Parry, J. M. Wouters, D. M. Moltz,† and Joseph Cerny

Department of Chemistry and Lawrence Berkeley Laboratory, University of California, Berkeley, California 94720

(Received 22 July 1980)

Beta-delayed protons have been observed from the decays of the mass separated $T_z = -2$ nuclides ^{20}Mg , ^{24}Si , and ^{36}Ca . From these proton spectra the mass excesses of the lowest $T = 2$ states in the $T_z = -1$ nuclei ^{20}Na , ^{24}Al , and ^{36}K are determined to be 13420 ± 50 keV (^{20}Na), 5903 ± 9 keV (^{24}Al), and -13168 ± 22 keV (^{36}K). The complete $A = 20, 24$, and 36 isospin quintets have all their members bound against isospin allowed particle-decay modes, providing a stringent test of the isobaric multiplet mass equation. Good agreement is observed for all these quintets using only the quadratic form of this equation.

[RADIOACTIVITY ^{20}Mg , ^{24}Si , ^{36}Ca (mass separated); measured β -delayed protons; deduced $T_{1/2}$ and proton branching; derived mass excesses of the lowest 0^+ , $T = 2$ states in ^{20}Na , ^{24}Al , and ^{36}K ; deduced coefficients of the isobaric multiplet mass equation.]

I. INTRODUCTION

Recent progress in studies of very proton-rich nuclides near the proton drip line has greatly been advanced by the development of accelerators and instrumentation techniques. An increasing component of our knowledge on exotic light nuclei is derived from the analysis of mass separated radioactivity¹; these studies can delineate the limits of nuclear existence in addition to providing basic information on the spectroscopy of nuclei far from stability.

Isobaric multiplets play a significant role in predicting masses of highly proton-rich light nuclides in addition to contributing to our basic understanding of charge dependent effects in nuclear forces. The masses of analog states in an isospin multiplet are given in first order by a quadratic relationship, introduced by Wigner in 1957, as follows²:

$$M(A, T, T_z) = a(A, T) + b(A, T)T_z + c(A, T)T_z^2.$$

This isobaric multiplet mass equation (IMME) arises via first order perturbation theory from the assumptions that the wave functions of the members of an isospin multiplet are identical and that only two body forces are responsible for charge dependent effects in nuclei. Possible deviations from this quadratic form can be due to higher order Coulomb or other charge dependent effects as well as to various isospin mixing effects (see also Ref. 3). These deviations are generally represented by the additional terms $d(A, T)T_z^3$ and $e(A, T)T_z^4$, in which the d and e coefficients can be derived from second order perturbation theory. These deviations can be studied only with isospin multiplets having $T \geq \frac{3}{2}$.

Extensive studies of isospin quartets have led to the observation of excellent agreement with the quadratic form of the IMME. However, a persistent deviation has been observed for the lowest mass 9 quartet.³ This significant result has partly been explained by the expansion of the least bound proton orbit in ^9C as well as by non-Coulombic charge dependent forces⁴; however, a fully satisfactory explanation has not been given so far.

Until fairly recently experimental information on the masses of certain members of isospin quintets was rather limited.³ Although mass excesses of the lowest $T = 2$ states in the $T_z = 0, +1$, and $+2$, $A = 4n$, nuclei were well-known starting with $A = 8$, difficulties were associated with mass determinations of the $T = 2$ states in the $T_z = -1$ and -2 nuclei. In only one case, the $A = 8$ quintet, were the mass excesses of all the members precisely determined.^{5,6} A deviation from the quadratic form of the IMME was observed in these mass 8 results, being at least partly attributable to the strong Coulombic repulsion in its particle unbound members as well as to isospin mixing in the $T_z = 0$ member of this quintet. As such, studies of higher mass quintets in which all members are bound to isospin-allowed particle decay modes are of particular interest.

Our research has focused on measurements of the mass excesses of the lowest $T = 2$ states in the $T_z = -1$ members of isospin quintets. These $T = 2$ states could, in principle, be located by using the isospin conserving (^3He , ^6He) reaction. However, the generally nonselective population by this reaction of both $T = 1$ and $T = 2$ states in the product nucleus limits its use to only a few cases. Another possible approach, adopted in this work, is the investigation of the β^+ -delayed proton decays of

the $T_z = -2$ nuclei produced via ($^3\text{He}, 3n$) and ($^3\text{He}, \alpha 3n$) reactions with even $Z=N$ target nuclides. These β^+ decays are highly selective in populating the $T=2$ analog state in the daughter nucleus via a superallowed beta-decay branch.⁷ However, because of simultaneous production of other strong β^+ -delayed proton emitters, on-line mass analysis of nuclides of different chemical nature and with half-lives as short as 50 ms would be required. In order to accomplish this, an instrument known as RAMA,⁸ for recoil atom mass analyzer, was constructed and will be described below.

In this paper we report the results from studies of the decays of the mass separated $T_z = -2$, $A = 4n$, nuclei ^{20}Mg ,⁹ ^{24}Si ,¹⁰ and ^{36}Ca . The beta-delayed proton spectrum for each nucleus was measured and the location of the lowest $T=2$ state in the $T_z = -1$ daughter nucleus was determined. Since members of these quintets are bound against isospin allowed particle decay, an important test of the quadratic isobaric multiplet mass equation is provided.

II. EXPERIMENTAL METHOD

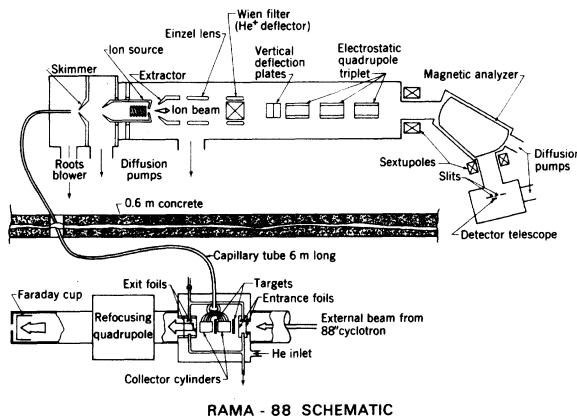
Beams of ^3He ions with energies from 40 to 100 MeV produced with the Berkeley 88-inch Cyclotron were used in these experiments. The $T_z = -2$ nuclei ^{20}Mg , ^{24}Si , and ^{36}Ca were produced via the ($^3\text{He}, 3n$) and ($^3\text{He}, \alpha 3n$) reactions using targets of natural Ne, Mg, and Ca. The beta-delayed proton decay of the mass separated nuclides was detected by a silicon surface-barrier detector telescope.

The recoils from the targets are thermalized in 1.3–1.5 atmospheres of helium and are collected by a multiple capillary system (see Figs. 1 and 2). A larger single capillary is used to transport the activity into the hollow-cathode ion source of the mass separator. Helium is pumped off

using a large Roots blower in conjunction with a skimmer system. Ionized recoils are extracted from the ion source using an 18 kV potential and are subsequently passed through a series of optical elements to focus the extracted beam before it is mass analyzed. A velocity filter is used ahead of the analyzing magnet to divert the strong helium beam produced by the arc support gas and hence to reduce any space charge problems. Typically, the total transit time for the recoils through this system is approximately 280 ms.

Our standard hollow-cathode ion source was used in the ^{20}Mg and ^{24}Si experiments while a new, but similar, ion source was developed for the ^{36}Ca experiments, since our standard source did not produce calcium in sufficient yield. The position of the arc and the filament are inverted in the new source (see Fig. 3) resulting in a longer and smaller diameter plasma compared to our normal source. The higher plasma density and longer confinement time resulted in a substantial increase in the ^{36}Ca and ^{37}Ca yields.

A high geometry (30% of 4π) silicon surface barrier detector telescope system was developed for the detection of the short lived $T_z = -2$ beta-delayed proton precursors. The detector configuration includes a $50 \mu\text{g}/\text{cm}^2$ carbon foil on which the mass separated ion beam of interest is implanted. The carbon foil is placed at 3 mm distance from the 1.5 cm diameter ΔE detector, which is directly followed by a 2.3 cm E detector. Thicknesses of ΔE detectors were varied from 25 to 44 μm while the thickness of the E detector was kept at a constant value of 300 μm . A typical energy resolution of about 55 keV full width at half maximum (FWHM) was achieved with a minimum threshold of about 1.5 MeV for detecting protons. An additional second detector telescope was installed on the focal plane at the next higher mass



RAMA - 88 SCHEMATIC

FIG. 1. Schematic view of the on-line mass separator system, RAMA.

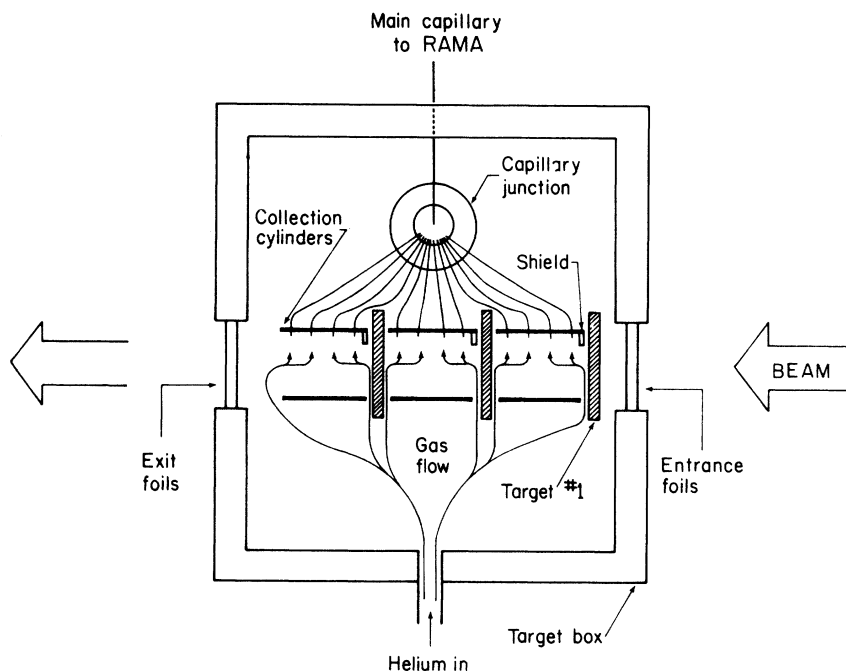


FIG. 2. The multiple-target-multiple-capillary system. The length of a collection cylinder approximates the maximum range of the recoil nuclei.

position. This provided a very convenient way to monitor the operation of RAMA via detecting the beta-delayed protons from the $T_z = -\frac{3}{2}$ nuclide of the element of interest.

Each telescope used a standard slow coincidence network together with fast timing between the ΔE

and E detectors; the timing resolution of this time-to-amplitude converter (TAC) was typically better than 15 ns (FWHM). Multiparameter data were recorded event by event on a Mod Comp IV Computer.¹¹ The parameters of interest for each telescope were the ΔE and E coincidence spectra, a TAC spectrum, and a ΔE anticoincidence spectrum.

The detector calibrations and the separation yields for each element were determined using the well-known beta-delayed proton emitters ^{21}Mg (Ref. 12), ^{25}Si (Refs. 10, 13), and ^{37}Ca (Ref. 13). As examples, the spectra resulting from the decays of ^{21}Mg and ^{37}Ca are shown in Figs. 4 and 5. In both of these cases the counting rates on the focal plane were typically between 0.5 and 2 counts/min at an average ^3He beam intensity of $5 \mu\text{A}$. Both spectra possess a pileup effect, which occurs as a small peak just above each major proton group. This effect is due to the simultaneous detection of a positron in the E detector and a proton in the telescope.

III. RESULTS

A. Decay of ^{20}Mg

The beta-delayed proton decay of ^{20}Mg was studied via the $^{20}\text{Ne}(^3\text{He}, 3n)^{20}\text{Mg}$ reaction at 70 MeV bombarding energy using spark chamber gas

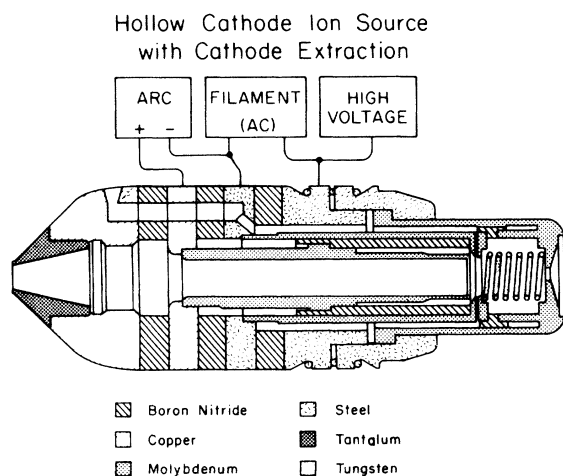


FIG. 3. The ion source developed for the ^{36}Ca experiment. Typically this source was run with a power of $250 \text{ V} \times 2 \text{ A}$ in the helium supported arc.

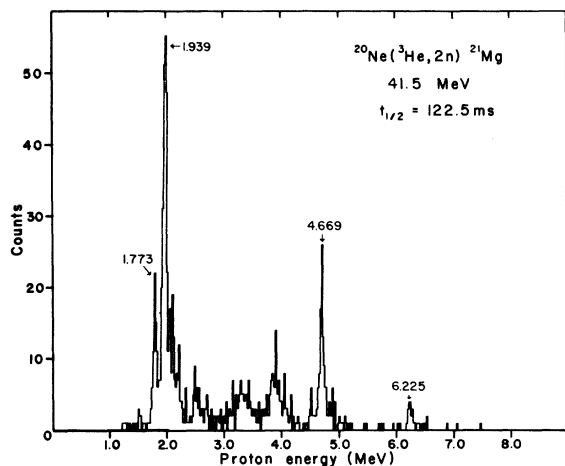


FIG. 4. A spectrum of beta-delayed protons from 122 msec ^{21}Mg . The lower yield peaks observed just above the major groups are sum peaks due to the simultaneous detection of a proton with its preceding positron.

(90% Ne and 10% He) both as a target and as a transport medium.⁹ After skimming, the ^{20}Mg activity was fed into our standard hollow-cathode ion source operated at about 1300 °C. Singly-charged, mass-analyzed ion beams were then directed onto a 2 μm thick foil of aluminized polyethylene in the focal plane; collected activity was observed by a semiconductor counter telescope. (In later experiments on ^{24}Si and ^{36}Ca this relatively thick foil was replaced by a thinner carbon foil.)

The proton spectrum arising from the decay of

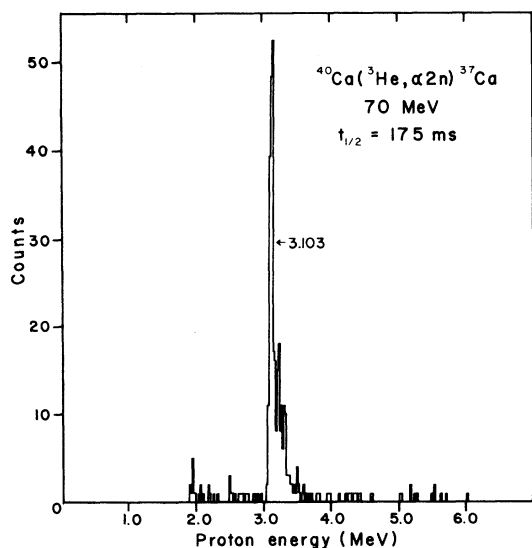


FIG. 5. The spectrum of beta-delayed protons from 175 msec ^{37}Ca . See caption to Fig. 4.

^{20}Mg after bombardment for 700 mC is shown in Fig. 6. The groups at 4.16 ± 0.05 and 3.95 ± 0.06 MeV are attributed to the isospin forbidden proton decay of the lowest 0^+ , $T=2$ state in ^{20}Na fed in the superallowed beta decay of the 0^+ , $T=2$ ground state of ^{20}Mg . Allowed beta decay to other states near this excitation energy would lead to considerably lower intensities in the proton spectrum. (The observed peaks cannot arise from the possible β -delayed proton decay of ^{20}Na since the maximum available energy in this decay is only 0.99 MeV.) A half-life of 95^{+80}_{-50} ms was observed for these peaks resulting in a branching ratio of $3 \pm 2\%$ for the superallowed decay ($\log ft = 3.18$). The center of mass energy of the more energetic proton group taken together with the ^{19}Ne mass excess⁴⁹ yields a mass excess of 13.42 ± 0.05 MeV for the lowest 0^+ , $T=2$ state in ^{20}Na .

The determination of the mass excess of the $T_z = -1$ member in the $A=20$ quintet completes the lightest quintet in which all members of the multiplet are bound against isospin allowed particle decay modes. The mass values of all the members in this quintet are given in Table I; this table includes the fits to the second, third, and fourth order polynomials to check the validity of the isobaric multiplet mass equation. An excellent fit ($\chi^2 = 1.02$) is obtained by using only the quadratic form, reflecting the insignificance of charge-dependent mixing, unlike the results obtained in the mass 8 multiplet.^{5,6}

B. Decay of ^{24}Si

The $^{24}\text{Mg}(^3\text{He}, 3n)$ reaction was used to study the decay of ^{24}Si .¹⁰ Three 1.2 mg/cm² natural Mg

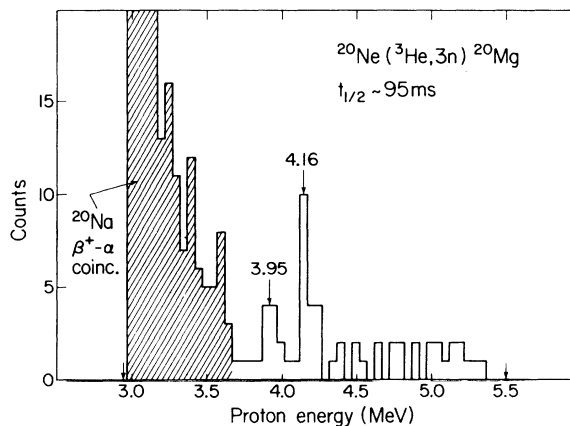


FIG. 6. The spectrum of beta-delayed protons from ^{20}Mg after bombardment for 700 mC. This spectrum is a combination of three separate runs. The high background at lower energies is associated with the strong β^+ -delayed α -emitter ^{20}Na .

TABLE I. Properties of the $A=20$ isobaric quintet and coefficients of the IMME.

| Nucleus | T_z | Mass excess (MeV) | E_x (MeV) | References |
|------------------|-------|----------------------|------------------|------------|
| ^{20}Mg | -2 | 17.57 ± 0.03 | 0 | 14 |
| ^{20}Na | -1 | 13.42 ± 0.05 | 6.57 ± 0.005 | 9 |
| ^{20}Ne | 0 | 9.6908 ± 0.0023 | 16.6908 ± 0.0023 | 15,16,17 |
| ^{20}F | +1 | 6.503 ± 0.003 | 6.519 ± 0.003 | 18 |
| ^{20}O | +2 | 3.799 ± 0.008 | 0 | 19 |

| Coefficients for the IMME: $M = a + bT_z + cT_z^2 + dT_z^3 + eT_z^4$ | | | | | χ_ν^{2a} |
|--|-------------|-------------|-------------|-------------|-----------------|
| a | b | c | d | e | |
| 9.6917(22) | -3.4372(51) | 0.2466(33) | | | 1.02 |
| 9.6909(23) | -3.4348(56) | 0.2489(39) | -0.0022(20) | | 0.77 |
| 9.6908(23) | -3.4441(74) | 0.2589(101) | | -0.0025(19) | 0.36 |
| 9.6908(23) | -3.464(33) | 0.278(34) | 0.005(9) | -0.007(9) | |

^aReduced $\chi_\nu^2 \equiv \chi^2/\nu$, where ν is the number of degrees of freedom.

targets were bombarded with a 6 μA , 70 MeV ^3He beam. Because of the highly nonvolatile nature of silicon, a high temperature hollow-cathode ion source with anode extraction was used in this experiment. This ion source, operated at about 1800 °C, produced a total ionization efficiency of about 0.1% for Si.

The proton spectrum arising from the decay of ^{24}Si after bombardment for 560 mC is shown in Fig. 7. Only one peak in the spectrum is evident, occurring at a laboratory energy of 3914 ± 9 keV. This peak, attributed to proton emission following the superallowed beta decay of the 0^+ , $T=2$ groundstate of ^{24}Si , cannot arise from the decay of ^{24}Al or $^{24}\text{Al}^m$ collected at the same mass position, because the maximum available proton energies in these latter decays are only 2.1 and 2.5

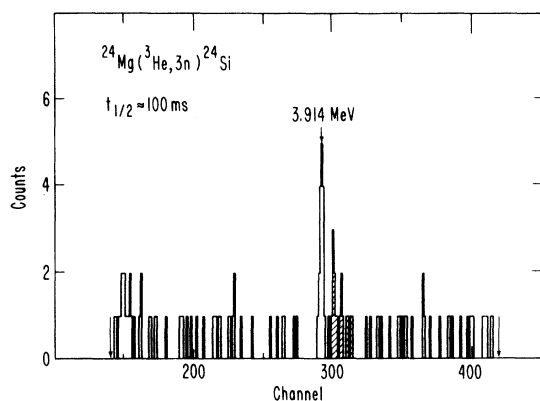


FIG. 7. The spectrum of beta-delayed protons from ^{24}Si after bombardment for 560 mC. The shaded counts above the group at 3.914 MeV are sum counts due to the simultaneous detection of a proton with its preceding positron.

MeV, respectively.¹⁹ A half-life of 100_{-40}^{+90} ms for ^{24}Si was estimated by comparing the experimental relative yields of ^{24}Si , ^{25}Si , ^{24}Al , $^{24}\text{Al}^m$, and ^{20}Na to those calculated with the OVERLAD ALICE code after correcting for the known system delay time. A branching ratio of $7_{-4}^{+6}\%$ was deduced for the superallowed beta branch based on the calculated $\log ft$ value of 3.18 and on the ^{24}Si ground state mass, 10.782 ± 0.022 MeV, measured recently by Tribble *et al.*²¹

Experimental mass values for the now complete $A=24$ quintet are given in Table II. The result of the most recent measurement of the beta delayed protons of ^{24}Si by Ledebuhr *et al.*²⁰ is included in this table; their experiment yielded a laboratory energy of 3911.2 ± 3.7 keV for the proton group deexciting the 0^+ , $T=2$ analog state in ^{24}Al . The weighted average of the proton energy, 3911.6 ± 3.4 keV in the center of mass system, taken together with the ^{23}Mg mass excess¹⁹ yields a mass excess of 5901.5 ± 3.9 keV for the lowest 0^+ , $T=2$ state in ^{24}Al . This multiplet, being the most precisely measured quintet thus far, provides an excellent test of the validity of the quadratic isobaric multiplet mass equation. All sets of IMME coefficients show no significant deviation from the quadratic form.

C. Decay of ^{36}Ca

The heaviest $T_z = -2$ nucleus studied in this work, ^{36}Ca , was produced via the $^{40}\text{Ca}(^3\text{He}, \alpha 3n)$ reaction at 95 MeV beam energy, using three 3 mg/cm² natural calcium targets. In earlier experiments on both ^{37}Ca and ^{36}Ca significant difficulties were encountered because the ionization efficiency of our standard ion source for Ca was much lower than for Si and Mg. A new ion source with higher plasma density as well as with a longer

TABLE II. Properties of the $A=24$ isobaric quintet and coefficients of the IMME.

| Nucleus | T_z | Mass excess (MeV) | E_x (MeV) | References | |
|--|-------------|----------------------|----------------------|------------|-----------------|
| ^{24}Si | -2 | 10.782 \pm 0.022 | 0 | 21 | |
| ^{24}Al | -1 | 5.9015 \pm 0.0039 | 5.9535 \pm 0.0056 | 10, 20 | |
| $^{24}\text{Mg}^a$ | 0 | 1.5014 \pm 0.0015 | 15.4320 \pm 0.0017 | 22-25 | |
| ^{24}Na | +1 | -2.4473 \pm 0.0012 | 5.9072 \pm 0.0009 | 27 | |
| ^{24}Ne | +2 | -5.949 \pm 0.010 | 0 | 19 | |
| Coefficients for the IMME: $M = a + bT_z + cT_z^2 + dT_z^3 + eT_z^4$ | | | | | |
| a | b | c | d | e | χ_ν^{2b} |
| 1.5014(14) | -4.1752(18) | 0.2264(19) | | | 0.86 |
| 1.5010(14) | -4.1734(25) | 0.2269(20) | -0.0017(16) | | 0.65 |
| 1.5014(15) | -4.1753(19) | 0.2264(32) | | 0.0000(10) | 1.71 |
| 1.5014(15) | -4.1716(34) | 0.2247(35) | -0.0028(21) | 0.0010(13) | |

^aThe mass excess value of 1505.8 \pm 0.9 keV, given in Ref. 26, was not adopted here because it differs from the given average number by as much as 4.4 keV.

^bReduced $\chi_\nu^2 = \chi^2/\nu$.

ionization region was thus constructed. With this source, an ionization efficiency for Ca equal to that of the standard source for Si and Mg was obtained. A counting rate of about 0.5 counts/min for the beta-delayed protons from ^{37}Ca decay was observed. Comparison of this rate to the somewhat better than 2 counts/min rate observed for ^{24}Mg and ^{25}Si indicates the cross section for production of ^{37}Ca is approximately 5 times lower than that for ^{24}Mg and ^{25}Si if similar He-jet efficiencies are assumed.

The ^{36}Ca experiment was made exceptionally difficult both by the expected very low yield and by possible interference from beta-delayed protons from the decay of ^{36}K . The maximum available proton energy in the latter decay is 4.18 MeV, while the predicted energy for the proton group following the superallowed beta decay of ^{36}Ca is about 2.56 MeV. Fortunately, a careful study of the decay of the very weak β -delayed proton emitter ^{36}K by Eskola *et al.*²⁸ is available and its spectrum is shown in Fig. 8(c). Their results show a number of alpha groups (shaded in the figure) as well as two proton groups at 2458 \pm 10 keV and 2640 \pm 10 keV [shown in Fig. 8(c)]; no evidence for proton groups between these two energies is seen.²⁸

Two experiments with different ion source conditions were performed at the mass 36 position on the focal plane of the mass separator. In both cases the yield of beta-delayed protons from the decay of the well-known nuclide ^{37}Ca in the counter telescope at the next higher mass position served as a monitor. First, to reproduce the ^{36}K results, the ion source was operated in a relatively cool mode to optimize production of potassium activities

relative to calcium activities. As is shown in the beta-delayed proton spectrum presented in Fig. 8(b), good agreement with the results of Eskola *et al.*²⁸ was obtained for the proton groups in the region of interest (only proton groups were observable in the counter telescope).

Second, the ion source was operated in a higher temperature mode with maximum possible filament and arc power to attempt to optimize ^{36}Ca production relative to the potassium yield. The beta-delayed proton spectrum from this experiment is shown in Fig. 8(a). Note that in the left hand side of this figure the yield of the "strong" proton group from ^{36}K at 0.97 MeV [observed by Eskola as shown in Fig. 8(c) and then by us in the experiments leading to Figs. 8(b) and 8(a)] is reduced by a factor of ~ 4 relative to that shown in Fig. 8(b) after accounting for integrated beam in the "high temperature" run as compared to the "cooler" run. The data of Fig. 8(a) show a new proton group at an energy of 2519 \pm 21 keV which we attribute to the superallowed beta decay of the 0^+ , $T=2$ ground state of ^{36}Ca to the 0^+ , $T=2$ state in its ^{36}K daughter followed by proton emission. Normal allowed beta decay leading to other proton emitting states would have too low a yield to be observable under present conditions.

The observed proton energy of 2519 keV taken in the center of mass system together with the mass¹⁹ of ^{35}Ar yields a value of -13168 \pm 22 keV for the mass excess of the lowest 0^+ ($T=2$) state in ^{36}K . A half-life of ≈ 100 ms was deduced using the known RAMA transit time and then comparing the experimental ratio of the yields of ^{36}Ca and ^{37}Ca with the calculated ratio obtained with the OVERLAD ALICE code. The beta-decay branching to

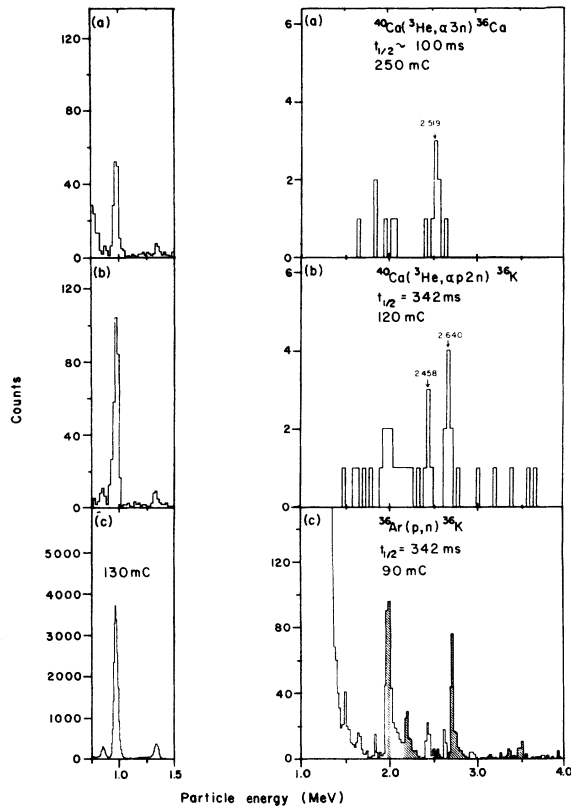


FIG. 8. (a) Right hand side: The spectrum of beta-delayed protons observed in a counter telescope at the mass 36 position after bombardment for 250 mC using the maximum ion source power. The peak at 2519 ± 21 keV is assigned to the decay of ^{36}Ca . Left hand side: Low energy (proton) groups observed in the telescope ΔE counter only. (b) Right hand side: The spectrum of beta-delayed protons observed at the mass 36 position after bombarding for 120 mC using the "cooler" ion source conditions. The peaks appearing in this spectrum are assigned to the decay of ^{36}K . Left hand side: Low energy (proton) groups observed in the telescope ΔE counter only. (c) Right hand side: The spectrum of beta-delayed protons and alpha-particles (shaded) obtained in a single counter from the decay of ^{36}K produced in the $^{36}\text{Ar}(p,n)$ reaction at 20 MeV (see Ref. 28). No protons were observed in the energy interval which would interfere with the group attributed to ^{36}Ca decay [part (a)]. Left hand side: Low energy (proton) groups observed in a single detector.

the $0^+(T=2)$ state was taken to be $\approx 20\%$ from the systematics of decays of other known $T_z = -2$ and $-\frac{3}{2}$ nuclei. Figure 9 presents the decay scheme deduced for ^{36}Ca ; the total decay energy shown uses the recent mass measurement for ^{36}Ca by Tribble *et al.*²¹ and the 1977 Mass Tables.¹⁹

The determination of the mass excess of the lowest $T=2$ state in ^{36}K completes the $A=36$ isospin quintet, thereby establishing the fourth com-

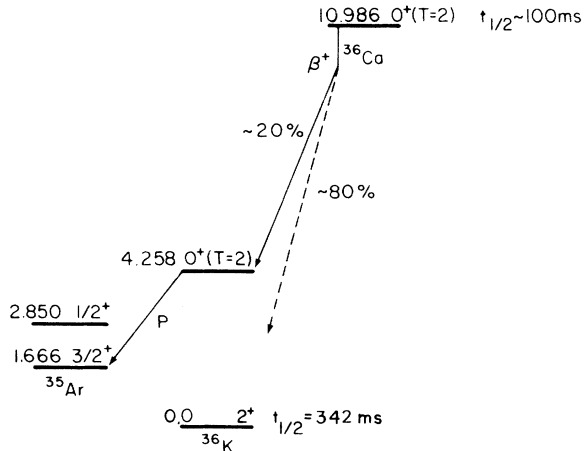


FIG. 9. A proposed decay scheme for ^{36}Ca .

pletely known quintet. Table III gives the masses of all members of this quintet (Refs. 29–34) together with the fits to the isobaric multiplet mass equation. The mass excess of the $T_z = 0$ member ^{36}Ar was obtained as an average of two published values, -19377.1 ± 1.6 keV (Ref. 30) and -19381.6 ± 1.5 keV.³¹ Since these numbers deviate from each other by more than their errors would indicate, the final error ± 2.2 keV was calculated with the method used by the Particle Data Group.³⁵ The same procedure was also applied to the final evaluation of the mass of the $T_z = \pm 1$ member, ^{36}Cl . The best fit to the data is again seen to be the quadratic IMME, although the reduced χ^2 indicates a poorer fit than that observed in the mass 20 and 24 quintets. Four parameter fits result in a d or an e coefficient consistent with zero. More precise measurements of the ^{36}Ca and ^{36}K points are necessary to determine any possible significance of the nonzero d and e coefficients found in the five parameter fit.

IV. DISCUSSION

The present study of the lowest $T=2$ states in the $T_z = -1$ nuclei ^{20}Na , ^{24}Al , and ^{36}K together with some other recent work on the $A=4n$ isospin quintets provides an exacting test for the isobaric multiplet mass equation beyond the well-known isospin quartets. The quintets with $A=28$ and 40 have only three of their members known; all other $2s1d$ shell $A=4n$ quintets have four or more precisely known members. Despite the experimental progress, very few calculations have been made to search for possible deviations from the quadratic form of the IMME. Shell model approaches both in an exact and in a perturbation theory treatment have been used to estimate the magnitude of a possible d coefficient in isospin quartets³

TABLE III. Properties of the $A=36$ isobaric quintet and coefficients of the IMME.

| Nucleus | T_z | Mass excess (MeV) | E_x (MeV) | References |
|------------------|-------|-----------------------|----------------------|------------|
| ^{36}Ca | -2 | -6.440 \pm 0.040 | 0 | 29 |
| ^{36}K | -1 | -13.168 \pm 0.022 | 4.258 \pm 0.023 | This work |
| ^{36}Ar | 0 | -19.3795 \pm 0.0022 | 10.8518 \pm 0.0022 | 30, 31 |
| ^{36}Cl | +1 | -25.2229 \pm 0.0013 | 4.2989 \pm 0.0013 | 34 |
| ^{36}S | +2 | -30.6659 \pm 0.0015 | 0 | 19 |

| Coefficients for the IMME: $M = a + bT_z + cT_z^2 + dT_z^3 + eT_z^4$ | | | | | |
|--|-------------|------------|-------------|------------|---------------------------|
| a | b | c | d | e | χ_ν^2 ^a |
| -19.3795(20) | -6.0437(37) | 0.2003(16) | | | 1.90 |
| -19.3801(22) | -6.0446(40) | 0.2030(46) | -0.0011(17) | | 3.42 |
| -19.3795(22) | -6.0434(74) | 0.1997(92) | | 0.0001(14) | 3.80 |
| -19.3795(22) | -6.018(15) | 0.177(15) | -0.0097(50) | 0.0075(41) | |

^aReduced $\chi_\nu^2 \equiv \chi^2/\nu$.

and result in values between ± 1 and -1 keV.^{4,36,37} However, the large experimental d coefficient observed in the $A=9$ quartet has not been fully explained either by isospin mixing effects or by higher order Coulombic effects.

A summary of the present experimental status of the d and e coefficients in isospin quintets is given in Fig. 10 (Refs. 5-7, 9, 10, 38). Two fits to the mass equation including the dT_z^3 or the eT_z^4 term in addition to the quadratic form are shown. The purpose of this presentation is to demonstrate the possible deviations from the basic quadratic form (nonzero d) or to extract information about isospin mixing effects in the $T_z=0$ members of the *complete* quintets (nonzero e). In a completely known quintet any shift in the $T=2$

state of the $T_z=0$ member produces a nonzero e , but does not affect the d coefficient. Figure 10 shows that the only significant deviations from the quadratic form are observed in the mass 8 and mass 16 systems with the latter being statistically less significant. In the mass 8 quintet the observed nonzero d and e coefficients have been explained both by the strong Coulombic repulsion in its particle-unbound members and by the effect of isospin mixing in the $T_z=0$ member.^{5,6}

Unlike the mass 8, 12, and 16 systems, the quintets with $A \geq 20$ have all their members bound against isospin allowed particle decay and thus provide a more stringent check than the lighter quintets. The overall results with these higher mass quintets indicate no necessity for the introduction of d and e coefficients. Generally, the currently available data on isospin quintets support the validity of the simple quadratic mass equation and provide no evidence for substantial higher-order charge-dependent effects in the nuclear interaction. For more accurate information, higher precision in the case of each quintet would be required. However, it should be noted that although the presence of a charge dependent nuclear interaction may result in higher order terms in the IMME, it also could significantly affect the value of the cT_z^2 term.³⁹ Thus studies of the IMME also involve analysis of the b and c coefficients, which are closely related to the detailed structure of the analog states.

ACKNOWLEDGMENTS

The authors wish to thank Professor R. E. Tribble and Professor R. G. H. Robertson for their results prior to publication. We also wish to thank Professor K. Eskola and his group for providing their ^{36}K data for our use. Dr. M.

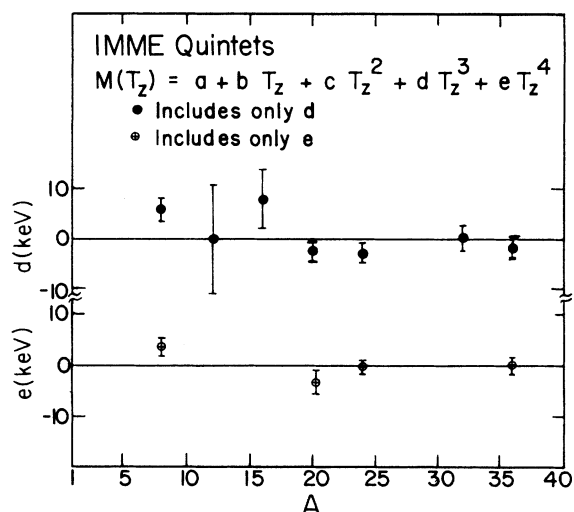
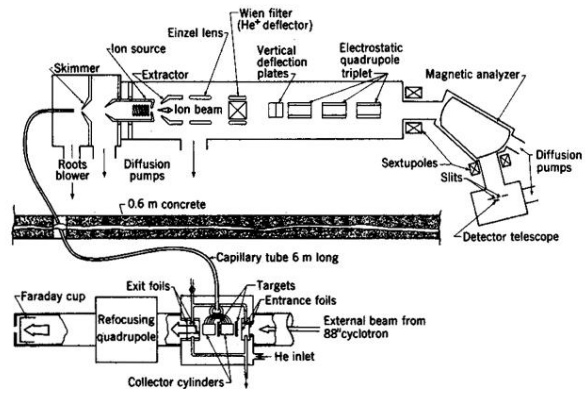


FIG. 10. The d and e coefficients of the IMME plotted as a function of the mass number of the quintet.

Blann kindly provided us with a copy of his evaporation code ALICE. This work was supported by the Nuclear Physics and Nuclear Science Di-

visions of the U.S. Department of Energy under Contract No. W-7405-ENG-48.

-
- *Present address: University of Jyväskylä, Department of Physics, Nisulankatu-78, Jyväskylä-72, Finland.
- †Present address: Physics Division, Oak Ridge National Laboratory, Oak Ridge, Tennessee.
- ¹Proceedings of the International Conference on Nuclei Far from Stability, Cargèse, 1976, Report No. CERN 76-13; and P. G. Hansen, *Ann. Rev. Nucl. Part. Sci.* **29**, 69 (1979).
- ²E. P. Wigner, in Proceedings of the Robert A. Welch Foundation Conference on Chemical Research, Houston, 1957, edited by W. O. Milligan, p. 67 (unpublished).
- ³W. Benenson and E. Kashy, *Rev. Mod. Phys.* **51**, 527 (1979).
- ⁴G. Bertsch and S. Kahana, *Phys. Lett.* **33B**, 193 (1970).
- ⁵R. G. H. Robertson, W. Benenson, E. Kashy, and D. Mueller, *Phys. Rev. C* **13**, 1018 (1976).
- ⁶R. E. Tribble, R. A. Kenefick, and R. L. Spross, *Phys. Rev. C* **13**, 50 (1976).
- ⁷E. Hagberg, P. G. Hansen, J. C. Hardy, A. Huck, B. Jonson, S. Mattsson, H. L. Ravn, P. Tidemand-Petersson, and G. Walter, *Phys. Rev. Lett.* **39**, 792 (1977).
- ⁸D. M. Moltz, R. A. Gough, M. S. Zisman, D. J. Vieira, H. C. Evans, and J. Cerny, *Nucl. Instrum. Methods* **172**, 507 (1980); D. M. Moltz, J. M. Wouters, J. Äystö, M. D. Cable, R. F. Parry, R. D. Von Dincklage, and J. Cerny, *ibid.* **172**, 519 (1980).
- ⁹D. M. Moltz, J. Äystö, M. D. Cable, R. D. von Dincklage, R. F. Parry, J. M. Wouters, and Joseph Cerny, *Phys. Rev. Lett.* **42**, 43 (1979).
- ¹⁰J. Äystö, D. M. Moltz, M. D. Cable, R. D. von Dincklage, R. F. Parry, J. M. Wouters, and J. Cerny, *Phys. Lett.* **82B**, 43 (1979).
- ¹¹C. Maples, Lawrence Berkeley Laboratory Report No. 9182.
- ¹²R. G. Sextro, R. A. Gough and J. Cerny, *Phys. Rev. C* **8**, 258 (1973).
- ¹³R. G. Sextro, Ph.D. thesis, University of California, Berkeley, Report No. LBL-2360, 1973.
- ¹⁴R. E. Tribble, J. D. Cossairt, and R. A. Kenefick, *Phys. Lett.* **61B**, 353 (1976).
- ¹⁵R. Block, R. E. Pixley, and P. Truol, *Phys. Lett.* **25B**, 215 (1967).
- ¹⁶H. M. Kuan, D. W. Heikkinen, K. A. Snover, F. Riess, and S. S. Hanna, *Phys. Lett.* **25B**, 217 (1967).
- ¹⁷E. G. Adelberger, A. B. McDonald, and C. A. Barnes, *Nucl. Phys.* **A124**, 49 (1969).
- ¹⁸G. F. Millington, R. M. Hutcheon, J. R. Leslie, and W. McLatchie, *Phys. Rev. C* **13**, 879 (1976).
- ¹⁹A. H. Wapstra and K. Bos, *At. Data Nucl. Data Tables* **19**, 175 (1977).
- ²⁰A. G. Ledebuhr, L. H. Harwood, R. G. H. Robertson, and T. J. Bowles, *Phys. Rev. C* **22**, 1723 (1980).
- ²¹R. E. Tribble, D. M. Tanner, and A. F. Zeller, *Phys. Rev. C* **22**, 17 (1980).
- ²²F. Riess, W. J. O'Connell, D. W. Heikkinen, H. M. Kuan, and S. S. Hanna, *Phys. Rev. Lett.* **19**, 367 (1967).
- ²³J. Szucs, B. Y. Underwood, T. K. Alexander, and N. Anyas-Weiss, *Nucl. Phys.* **A212**, 293 (1973).
- ²⁴J. L. Osborne, E. G. Adelberger, and K. A. Snover, *Nucl. Phys.* **A305**, 144 (1978).
- ²⁵A. B. McDonald, E. D. Earle, and W. McLatchie, *Nucl. Phys.* **A305**, 151 (1978).
- ²⁶J. C. P. Heggie and H. H. Bolotin, *Aust. J. Phys.* **30**, 407 (1977).
- ²⁷D. F. H. Start, N. A. Jelley, J. Burde, D. A. Hutcheon, W. L. Randolph, B. Y. Underwood, and R. E. Warner, *Nucl. Phys.* **A206**, 207 (1973).
- ²⁸K. Eskola, M. Riihonen, K. Vierinen, J. Honkanen, M. Kortelahti, and K. Valli, *Nucl. Phys.* **A341**, 365 (1980). See also G. T. Ewan, E. Hagberg, J. C. Hardy, B. Jonson, S. Mattsson, and P. Tidemand-Petersson, *ibid.* **A343**, 109 (1980).
- ²⁹R. E. Tribble, J. D. Cossairt, and R. A. Kenefick, *Phys. Rev. C* **15**, 2028 (1977).
- ³⁰A. Huck, G. J. Costa, G. Walter, M. M. Aleonard, J. Dalmas, P. Hubert, F. Leccia, P. Mennrath, J. Verotte, M. Langevin, and J. M. Maison, *Phys. Rev. C* **13**, 1786 (1976).
- ³¹D. J. Martin, H. C. Evans, and J. A. Szucs, *Phys. Rev. C* **14**, 1320 (1976).
- ³²D. J. Martin, J. A. Szucs, and D. T. Kelly, *Can. J. Phys.* **53**, 1734 (1975).
- ³³J. A. Rice, B. H. Wildenthal, and B. M. Preedom, *Nucl. Phys.* **A239**, 189 (1975).
- ³⁴J. Verotte, S. Fortier, M. Langevin, J. M. Maison, and M. Vergnes, *Phys. Rev. C* **13**, 461 (1976).
- ³⁵Particle Data Group, *Phys. Lett.* **50B**, (1974).
- ³⁶J. Janecke, *Nucl. Phys.* **A128**, 632 (1969).
- ³⁷E. M. Henley and C. E. Lacy, *Phys. Rev.* **184**, 1228 (1969).
- ³⁸G. J. KeKelis, M. S. Zisman, D. K. Scott, R. Jahn, D. J. Vieira, Joseph Cerny, and F. Ajzenberg-Selove, *Phys. Rev. C* **17**, 1929 (1978).
- ³⁹R. Sherr and I. Talmi, *Phys. Lett.* **56B**, 212 (1975).



RAMA - 88 SCHEMATIC

FIG. 1. Schematic view of the on-line mass separator system, RAMA.

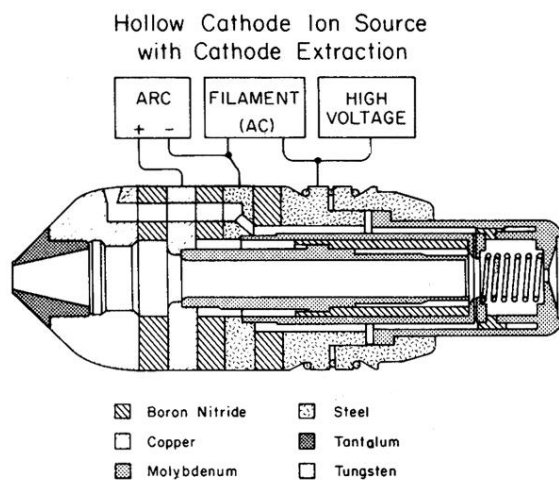


FIG. 3. The ion source developed for the ^{36}Ca experiment. Typically this source was run with a power of $250\text{ V} \times 2\text{ A}$ in the helium supported arc.